A Satellite-Derived UV Radiation Climatology over Europe to Support Impact Studies

Author: Verdebout, Jean

Source: Arctic, Antarctic, and Alpine Research, 36(3) : 357-363

Published By: Institute of Arctic and Alpine Research (INSTAAR), University of Colorado

URL: https://doi.org/10.1657/1523-0430(2004)036[0357:ASURCO]2.0.CO;2

Arctic, Antarctic, and Alpine Research, Vol. 36, No. 3, 2004, pp. 357–363

A Satellite-Derived UV Radiation Climatology over Europe to Support Impact Studies

Jean Verdebout

European Commission–Joint Research Centre, Institute for Health and Consumer Protection,
Via E. Fermi 1,
21020 Ispra (VA), Italy.
jean.verdebout@jrc.it

Abstract

The paper briefly presents a methodology for mapping surface UV radiation that uses a radiative transfer model and satellite data to quantify the influencing factors. TOMS, TOVS, and GOME data are used for the total column ozone. The cloud optical thickness is estimated using METEOSAT/MVIRI images. Other influencing factors taken into account include tropospheric aerosols, snow cover, and surface elevation. The resulting products are maps of surface dose rates and daily doses, covering Europe with a spatial resolution of 0.05°. On this basis, construction of a European UV climatology has been undertaken, with the purpose of supporting impact studies on the environment and human health. The data set covers the period from 1 January 1984 to 31 August 2003. A comparison between the satellite estimates and the measurements in Ispra, Italy, is briefly presented. Finally, examples of how the climatological data set can document the geographical distribution and year-to-year variability in surface UV radiation are presented.

Introduction

Exposure to high levels of UV radiation is harmful to human health (skin cancer, cataract, immuno-suppression), and it influences many natural biological processes (marine life, plant physiology). Our awareness of these effects has been raised by ozone depletion, which leads to an increase in the intensity of the UV radiation reaching the Earth surface in some regions of the world. The importance of monitoring the changes that occur in this environmental parameter is now recognized. Although ground radiometers will remain the reference in terms of accuracy, they are too few to offer a comprehensive geographical coverage. Consequently methods that aim to map the surface UV radiation intensity by combining modeling and satellite data are being developed. Global UV data sets have been generated from ozone satellite sensors such as TOMS (Eck et al., 1995; Krotkov et al., 1998, 2001), TOMS and ERBE (Earth Radiation Budget Experiment) (Lubin et al., 1998), and GOME (Global Ozone Monitoring Experiment) (Peeters et al., 1998). They are extremely useful for documenting the year-to-year variability and for detecting trends at large spatial scales (Ziemke et al., 2000). However, more specific UV impact assessments need information with a higher spatial resolution. This requires using additional data to describe better the spatial distribution of clouds, which can be the ISCCP (International Satellite Cloud Climatology Project) data (Slaper et al., 1998) or AVHRR-derived cloud optical thickness at 1-km resolution (Meerkötter et al., 1997). The work presented here is using the full resolution images from METEOSAT, the operational European geostationary weather satellite. Over Europe, the spatial resolution is typically 5 km (degrading at high latitudes because of the increasing viewing angle). METEOSAT acquires the Earth disk image every half-hour and thereby allows taking into account the high temporal dynamics of clouds when estimating daily doses; this is a specific advantage of the method.

UV Mapping Algorithm

The mapping methodology is described in detail elsewhere (Verdebout, 2000). To summarize, UV radiation maps over Europe (34°N–74°N, 12°W–32°E) are generated with a spatial resolution of 0.05°, and potentially on a half-hour basis. The surface UV dose rate is obtained by interpolation in a Look Up Table (LUT) of modeled irradiance, the entries of which are solar zenith angle, total column ozone amount, cloud optical thickness (COT), near surface horizontal visibility, surface elevation, and UV albedo. The LUT was computed with the UVspec code (Mayer et al., 1997) of the libRadtran package (version 13). Both satellite and nonsatellite (synoptic observations, meteorological model results, digital elevation model) data are exploited to assign values to the influencing factors. The total column ozone is extracted from the gridded TOMS data or other satellite ozone sensors data (e.g., TOVS, GOME). The aerosol optical thickness is tentatively taken into account by gridding daily measurements of near surface horizontal visibility performed at about 1000 ground stations. The digital elevation model is the GTOPO30 data set from United States Geological Survey (USGS).

With the help of another LUT simulating the "at sensor radiance" (proportional to the image digital count), METEOSAT data are processed to retrieve the cloud optical thickness. The calibration factor between the digital count and the values in the LUT has been empirically determined from the saturation values corresponding to very thick clouds. The entries of the METEOSAT signal LUT are solar zenith angle, METEOSAT viewing zenith angle, relative azimuth between illumination and viewing vectors, effective surface albedo, and cloud optical thickness. A preliminary step consists in generating an effective surface albedo map (in the MVIRI visible band) by finding cloud-free pixels in a series of 10 consecutive days. In most cases, the cloudless pixel is chosen as the one corresponding to the lowest signal in the visible band. However, if the surface is snow covered, the surface reflectance is high and the darkest visible signal does not necessarily indicate the absence of clouds. Therefore, if the effective surface reflectance is found to be above a certain threshold, the discrimination is refined by also using the thermal infrared band. The rationale for this second algorithm is that the pixel brightness temperature should be higher when cloud free than when cloud covered, even if snow is present. However, a threshold for discrimination can only be defined locally as the surface temperature varies considerably with geographical location. The land surface was

1523-0430/04 $7.00

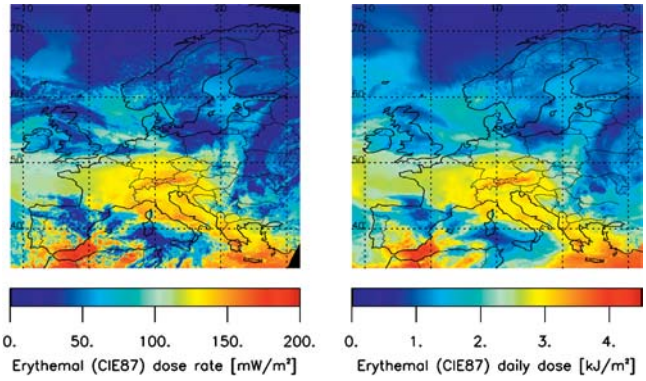

FIGURE 1. Erythemal dose rate at ~11:22 UTC and erythemal daily dose estimated with half-hourly METEOSAT images on 18 April 1997.

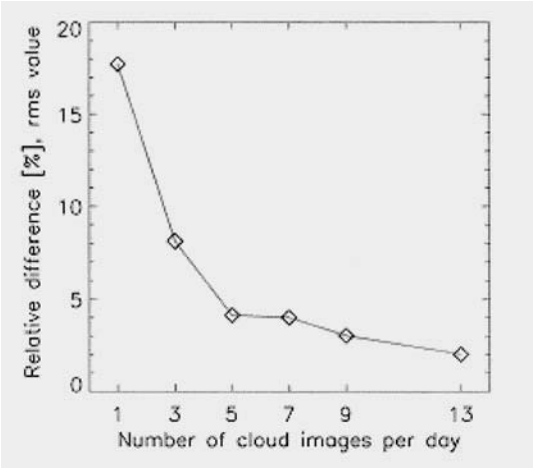

FIGURE 2. Dependence of the error on daily dose with respect to the number cloud images used per day.

therefore divided in 67 zones according to latitude and geophysical characteristics. In particular, the main mountainous areas (the Alps, the Pyrenees, the Caledonian range in Scandinavia) constitute such zones. In mountain areas, the zone is further subdivided in altitude classes. For each class, the histogram of the infrared METEOSAT brightness temperature over 10 days is fitted as a sum of Gaussian functions. The cloud free-pixels are associated with the "warmest" Gaussian and a threshold is determined on this basis. Once the composite cloudless digital count image has been constructed, it is transformed in an effective albedo map by inversion, using the LUT reduced to the cloudless case. The effective albedo map is then used to estimate the cloud optical thickness for the day and time of interest, by inversion using the full LUT. Most of the Earth surfaces are very dark in the UV spectral range, with the important exception of snow. Fresh snow can reflect almost 100% of the UV radiation and the induced increase in the surface radiation intensity in snow-covered areas is substantial. The UV surface albedo is therefore assigned uniform values for land (0.03) and sea/ocean (0.06), except in the presence of snow. In this case it is given a value proportional to the METEOSAT effective albedo. The rationale for proportionality between the albedos in the two spectral ranges is that partial snow cover should affect them in a similar way. The outputs of the METEOSAT processing are fed into the UV map processor to generate surface UV irradiance maps or dose rate maps when a spectral weight is applied.

As stated before, gridded daily visibility observations are used as a proxy for aerosol optical thickness (AOT). These input data are far from being ideal because, even with about 1000 stations, the geographically interpolated values are likely to be often quite different from reality. Furthermore low visibility can result from rain and not from high aerosol load. In the latter case, however, the impact on the surface UV irradiance is small in absolute terms because rain also implies fairly high cloudiness. These data are still used because a better suited information source is not available, at least for the 20-yr period and the area covered by the UV climatology. As the aerosols also contribute to the atmospheric optical thickness, one can also argue that they are included in the METEOSAT retrieved COT and taken into account twice. This is partly true. However, the minimal signal during 10 days also contains an aerosol fraction. As the METEOSAT LUT is constructed for an aerosol-free atmosphere this contribution is interpreted as part of the surface reflectance. Therefore, only a difference in aerosol optical thickness (AOT) is included in the COT, if large enough to be detected by the MVIRI instrument, which has a radiometric resolution of only 8 bits (or even 6 bits for the earlier instruments). One can think of adding the AOT as an entry of the LUT and taking it into account in the conversion of the minimal signal into a surface reflectance. This makes the LUT much bigger and has a high cost in processing time for a small or no improvement of the result (probably because the interpolated visibility values are not precise enough). Keeping with the present LUT and explicitly introducing the aerosols in the second step does introduce the large-scale systematic spatial difference in AOT over Europe and has been found to slightly improve the correlation with measurements at some stations.

The daily dose is constructed by numerical integration of the dose rate estimated at half-hourly intervals from and including the local solar noon (for each pixel). At each of these times, the solar zenith angle is computed and the cloud optical thickness is assigned a value. The other influencing factors (column ozone, surface albedo, aerosol optical thickness, and surface UV albedo) are considered constant. The COT time dependence is described with a stepwise function with as many time intervals as the number of METEOSAT images used per day. Using only one image means that the COT is constant. At the other extreme, if all METEOSAT images are used the COT value is sampled at half-hourly intervals. In METEOSAT terminology, the acquisitions are named slots, numbered from 1 to 48. Acquisition of slot 1 begins at 0:00 UTC and takes 25 min to complete, slot 2 acquisition starts at 0:30 and so on. As the Earth disk image acquisition starts from the south, Europe is imaged approximately at 22 min or 52 min past the hour, respectively, for odd and even slots (acquisition of the European area only takes ~4 min). Figure 1 shows the erythemal dose rate corresponding to slot 23 on 18 April 1997 (~11:22 UTC) and the dose for this day, reconstructed with half hourly images (Verdebout and Vogt, 2001). One can notice that the cloud pattern in the dose map is smoother than in the dose rate. This is expected from the movement of the clouds during the day.

With the method outlined above, construction of a European climatology of UV radiation has been undertaken. As of today it consists in daily dose maps from 1 January 1984 to 31 August 2003. For practical reasons (processing time and amount of data) one METEOSAT image per day only has initially been used. The data set is progressively upgraded to using three images per day; this is already the case for March and July from 1990. Figure 2 shows how the accuracy on daily dose is improved by using more images per day (Verdebout and Vogt, 2001). This estimate was obtained by comparing daily dose maps obtained with a variable number of images per day to the reference result with half-hourly cloud data. The statistical values reported in Figure 2 represent the error for a single day (18 April 1997) over the entire area covered by the map. This single map however contains a large variability in all influencing parameters (ozone, COT, snow cover, solar zenith angle, altitude, and aerosol load). It can be seen that using three images per day already largely improves the

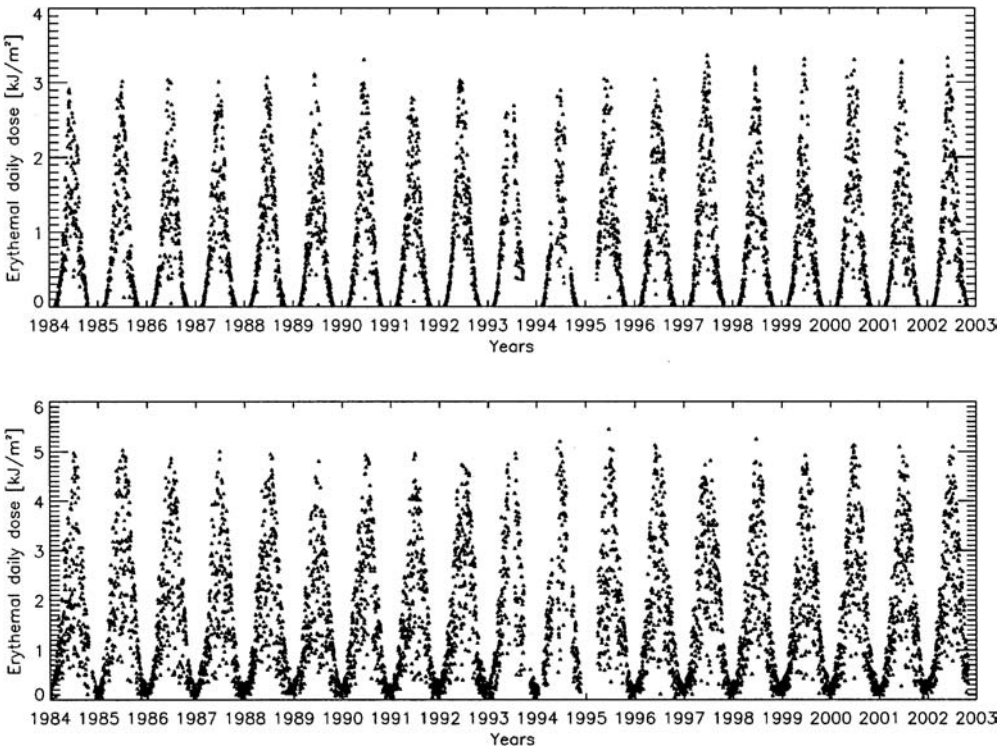

FIGURE 3. Time series of erythemal daily dose as extracted from the maps at Tromsø (top) and Garmisch-Partenkirchen (bottom).

results. Using five images per day would statistically bring this source of error below 5% and make it comparable to other uncertainties (e.g., those due to the error on total column ozone).

When covering the period from 1984, data from different instruments are used, in particular the four TOMS (and TOVS and GOME for limited periods) and METEOSAT 2 to 7. Inconsistencies and drifts (e.g., caused by instrument degradation) in these input data will translate in a spurious variability in the UV climatological data set. The same is true for visibility. To assess the potential impact, it is important to know the sensitivity of the UV model output with respect to uncertainties in the input data. The results of the sensitivity studies are not easily summarized with a few numbers because the effects of the various influencing parameters are strongly coupled. One can, however, say that an overestimation of 5% of the total column ozone produces an underestimation of 4 to 7% on the erythemal irradiance and of 8 to 15% if the DNA action spectrum (putting more weight on shorter wavelengths) is used. The impact on UVA irradiance is negligible. This spectral dependence of course results from the increase of the ozone absorption coefficient at shorter wavelengths. Artificially decreasing the gain of MVIRI by 5% leads to errors varying between –1% and +6% in most cases. The relative error can be much larger under very thick clouds. In this case, the MVIRI signal saturates and becomes almost insensitive with respect to the COT, the retrieved value of which is then critically affected by a change in the signal. In this case however, the absolute error on the surface irradiance is small as the irradiance itself is small. A more serious problem occurs when the change in the signal reverses the outcome of the snow/cloud discrimination. The error can then be huge. The sensitivity of the result with respect to the MVIRI dark signal is much less; an error of 1 digital count induces no more than a ±1% on the surface irradiance, except again when it provokes the reversal of the snow/cloud discrimination. Finally, an overestimation of the visibility by 5% induces an error of at most 1%. As expected, the errors related to the MVIRI signal and the visibility do not show any strong spectral dependence.

The most severe problem for the climatological dataset is posed by the changing gain of the MVIRI instruments, which can amount to 15% over the 1984–2003 period. This has been dealt with by devising a vicarious month-by-month equalization procedure. The principle of this procedure is that, over a sufficiently long period of time (e.g., one month), one should find pixels in the images that correspond to very thick clouds (high signal) and clear sky over ocean conditions (low signal) and then to assume that the top-of-atmosphere reflectance for these two extreme conditions are invariants (Verdebout and Vogt, 2001). Assessing the success of this equalization will need comparisons with long time series of ground measurements.

The maps have been generated for UVB, UVA, and PAR (Photosynthetically Active Radiation, 400–700 nm) spectral ranges and using the CIE87 erythemal action spectrum. However, the model output is spectral and the dose corresponding to any desired action spectrum can be generated on request. For instance, dose maps with the action spectra for cod eggs and zooplankton (*Calanus finmarchicus*) mortality were generated in the framework of the UVAC project. UVAC (UV and arctic cod) studied the influence of natural UV radiation on the populations of the northeast arctic cod (Hansen, 2003). The climatological data are available from JRC for scientific purpose (e.g., impact studies). The examples shown in this paper are all relative to erythemal doses, which are the most commonly used UV data.

The maps do not and cannot include the polar regions, which lie below the viewing horizon of a geostationary satellite. Actually, the accuracy of the UV mapping method is expected to degrade with higher latitude, where the METEOSAT pixel gets larger and distorted. The high solar illumination and viewing zenith angles also reduce the satellite signal dynamic range. The northernmost latitude of 74° is the practical limit for applying the method. Furthermore, the Arctic is an area where the difficult problem of distinguishing snow from clouds is often encountered. This is also the case in alpine regions. Useful results can nevertheless be obtained. Figure 3 shows two examples at a Nordic site (Tromsø, 69.662°N–18.942°E) and at an Alpine one (Garmisch-

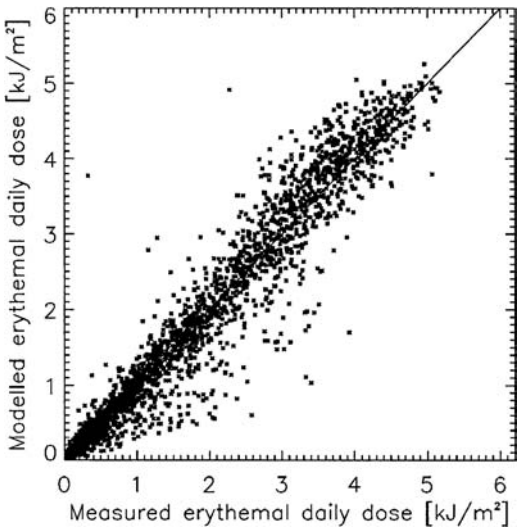

FIGURE 4. Comparison of satellite-derived and measured erythemal daily doses at Ispra (all available data from 1994 to 2003).

Partenkirchen, 47.48°N–11.07°E). These time series are typical of the data already delivered to projects dealing with impact studies. Spatially averaged daily doses over an area of interest can also be easily generated. About 10% of the days are missing either because of missing METEOSAT images (in the earlier years in particular) or because of lack of satellite ozone data (in the 1992–1995 period). In Tromsø, the daily dose is also systematically missing in a winter period, when the high solar zenith angle makes the model inapplicable. At high latitudes, the initial algorithm often yields unrealistically large COT values. This is attributed to the cloud structure and associated bi-directional reflectance, which makes them appear brighter at high solar and viewing angles. The results have been improved by empirically correcting the MVIRI signal. Angle-dependent gain and dark signal correction factors have been obtained by imposing that the COT of the thickest clouds and the lowest sea albedo, detected during a long period, minimally depend on the illumination and viewing angles (Meerkötter et al., 2002). These corrections are significant only for solar zenith angles exceeding ~75°.

With its additional spectral bands and increased radiometric resolution, MSG (Meteosat Second Generation) will substantially improve the results quality. MSG will replace the present METEOSAT in 2004. It should be mentioned that high spatial resolution UV radiation satellite estimates over the polar regions can be obtained using data from polar orbiting satellites (Meerkötter et al., 1997).

Comparison with Ground Measurements

Comparison between satellite estimates and ground measurements is best conducted on daily doses. The satellite estimate is by nature an average over a certain area (the map pixel) while the measurement is at a single point. The instantaneous measurement of surface irradiance is sensitive to the detailed cloud structure (it is for instance influenced by a small cloud obscuring the sun). The satellite-modeled value on the other hand corresponds to a uniform cloud reproducing the average cloud optical thickness over the area. The fact that the measurement and the satellite image acquisition are never perfectly simultaneous further complicates the comparison on irradiance. Because the clouds move, the time integration performed to estimate the daily dose from the measurements smoothes the cloud structure and has an effect similar to the spatial integration in the satellite image. Even so, part of the observed difference between the two data reflects their different nature. In order to compare with ground measurements, time series of daily doses in the pixel containing the ground station are extracted from the maps. Figure 4 shows a comparison between the measured and satellite-derived erythemal daily dose in Ispra (45.81°N–8.63°E, on the Lago Maggiore, in the Italian pre-Alps), in the form of a scatter plot. The data points include every day between 1994 and 2003 for which the satellite data and at least 20 irradiance measurements are available. The rms relative difference is 29% and the mean relative difference or bias +3% ([sat-ground]/ground). Figure 5 shows the measured and modeled monthly averaged erythemal daily dose from 1996 to 2003, the rms relative difference is here 7%. Such a comparison was also conducted in Tromsø, against measurements during March, April, and May from 1996 to 1999 (Meerkötter et al., 2003). Despite the previously mentioned difficulties related to the high latitude, the agreement is not very different (33% rms relative difference and –0.3% bias). The same study also contains a comparison with AVHRR-derived values at 1-km resolution (by DLR, Deutsches Zentrum für Luft-und Raumfahrt). The two algorithms are very similar, with AVHRR playing the role of MVIRI for COT estimation. Being on a polar orbiting platform, AVHRR does not suffer from high viewing zenith angles and keeps it full spatial resolution at high latitudes. The rms difference and bias were found to be 37% and +4.6%, respectively, for AVHRR-derived daily doses. Previous comparison results, but on the basis of only 1 yr of data (1997), have been obtained at Garmisch-Partenkirchen (Germany), Brussels (Belgium), Bilthoven (The Netherlands), and Jokioinen (Finland) (Arola et al., 2002). In this study, three other satellite methods (using AVHRR, ISCCP, and GOME) are also evaluated. The METEOSAT-derived erythemal daily doses showed, with respect to the measurements, rms difference of 31, 31, 32, and 37% and biases of –0.9, –6.2, –16.1, and –4.6%, respectively, in Garmisch-Partenkirchen, Brussels, Bilthoven, and Jokioinen. The corresponding numbers for the ISCCP-derived daily doses (by RIVM, National Institute of Public Health and the Environment of the Netherlands) are 37, 33%, 26, and 31% (rms differences) and –2.5, +11.6, –0.9, and +1.8% (biases). The GOME-based method (Belgian Institute for Space Aeronomy) did not perform as well but the algorithm was at an early stage of development. There were not enough data at the time to produce the statistics for the AVHRR-derived results. So far, there is no direct comparison with the TOMS UV data. The TOMS satellite retrievals have been found to

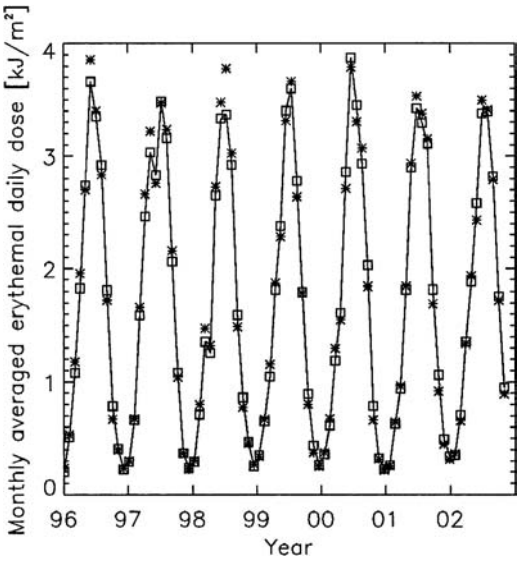

FIGURE 5. Monthly averaged erythemal daily dose in Ispra, from 1996 to 2003: squares and solid line represent the measured values, stars the satellite estimates.

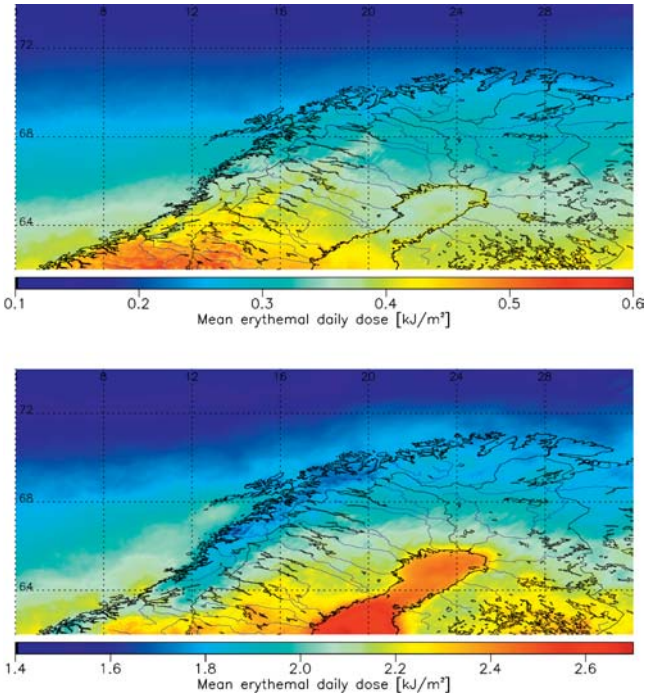

FIGURE 6. Multiyear (1984–2003) average of the daily erythemal dose over north Scandinavia/Finland; top: in March, bottom: in July.

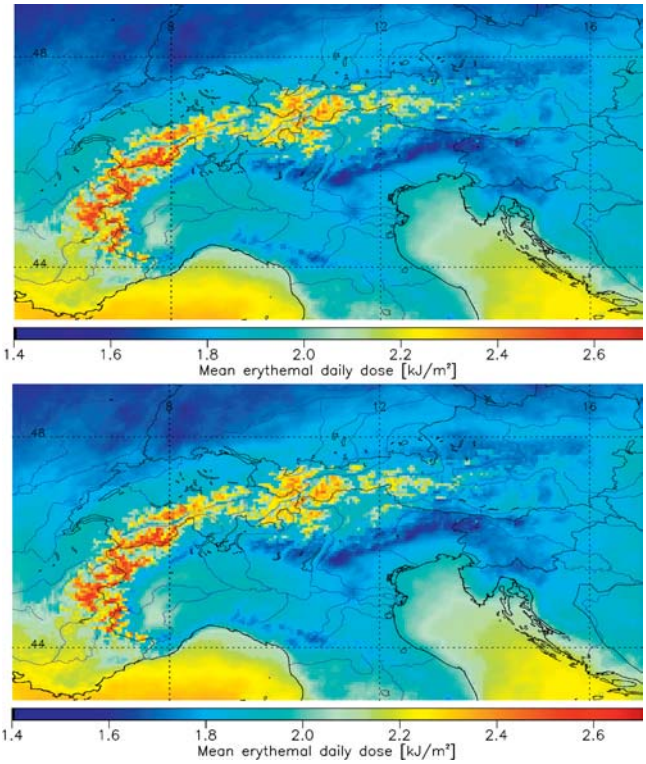

FIGURE 7. Multi-year (1984–2003) average of the daily erythemal dose over the Alpine arc: top—in April, bottom—in August.

show a quite systematic overestimation of the erythemal daily dose by 15 to 30%, at northern mid-latitudes (McKenzie et al., 2001). It is suspected that the main cause is a failure of the TOMS algorithm to correctly account for aerosol effects. In this regard, it should be stated that the TOMS algorithm is fundamentally different from the METEOSAT, AVHRR, and ISCCP methods. The TOMS algorithm is based on a radiation budget and infers the surface radiation from that backscattered and detected by the TOMS instrument. In this sense the TOMS results retain the character of a measurement. The other methods, which do not exhibit a systematic overestimation, are essentially direct modeling exercises where the tropospheric aerosols are explicitly introduced, even if imperfectly or even if constant climatological values are used. Finally, the differences with respect to the measurements must be evaluated against the absolute calibration precision of the ground instruments that can be stated to be about ±7% (Bernhard and Seckmeyer, 1999).

Examples from the Climatology

Systematic geographical features in the distribution of surface UV radiation are best identified in multi-year averages. Figures 6 and 7 show monthly averaged erythemal daily doses, themselves averaged from 1984 to 2003, over North Scandinavia/Finland and the Alpine arc for different months. The geographical distribution of the UV radiation is essentially related to latitude, altitude, presence of snow, and patterns in the cloudiness. In multi-year averages, the ozone distribution accounts at most (in spring) for a ~20% difference in the erythemal dose and over large spatial scales (within the European area covered by the maps). In Figure 6, the overall north-south gradient, much more pronounced in March than in July, is due to the solar zenith angle and daytime duration. In March, the higher values over the Caledonian range (for instance compared with Finland at the same latitude) is caused by the combined effects of altitude and snow cover, even if attenuated by a higher cloudiness over the mountains. In July, the most noticeable feature is the higher average UV radiation over the Gulf of Bothnia with respect to surrounding land (by ~15%). This is associated with a markedly lower cloudiness: the convective clouds form over the warmer land. One can also notice that this effect is not present in March, when the cloudiness is actually slightly higher over sea than over land. In July, the lower values on the Norwegian coast are caused by heavier cloudiness. Unfortunately barely distinguishable in the printed image, another small systematic enhancement of UV radiation over the coastal areas in the Gulf of Bothnia is due to the presence of sea ice in March. Similar effects are seen over the Alps: the enhancement by altitude and snow and the differences between land and sea (Fig. 7). Here too the cloudiness is higher over the mountains but over-compensated by altitude (and snow in April) in the highest regions. The effect of clouds is dominant in the pre-Alpine zones and over the Apennines. The contrast between land and sea is already present in April. In August, one can also notice the large difference between the Po valley and the region north of the Alps, caused by much heavier cloudiness in the north. In April on the contrary the cloudiness is comparable on both sides.

The data set also documents the year-to-year variability in UV radiation. Figures 8 and 9 show the deviation with respect to the 1984–2003 average of the monthly averaged erythemal daily dose over the Nordic area in March and the Alps in April. One can first notice that the variability is quite large, reaching –40% to +50%. Although some other factors (snow, aerosols) also contribute, the year-to-year differences are mostly related to the variability in total column ozone and cloudiness. Any combination is encountered. In Figure 9, the particularly high UV in April 1997 corresponds to low ozone (~ 310 DU) and low cloudiness; this high UV area actually extends over most of Europe (except the southeast). Inversely the low UV in the North in March 1989 or in the Alpine region in April 1989 corresponds to the conjunction of high ozone (~430 DU and ~380 DU, respectively) and high cloudiness. The lows in the North in March 1999 and in April 1991 in the Alpine area are entirely caused by particularly high values of ozone (up to 500 DU and up to 420 DU, respectively) while the cloudiness is in both cases one of the lowest in the series. The high UV

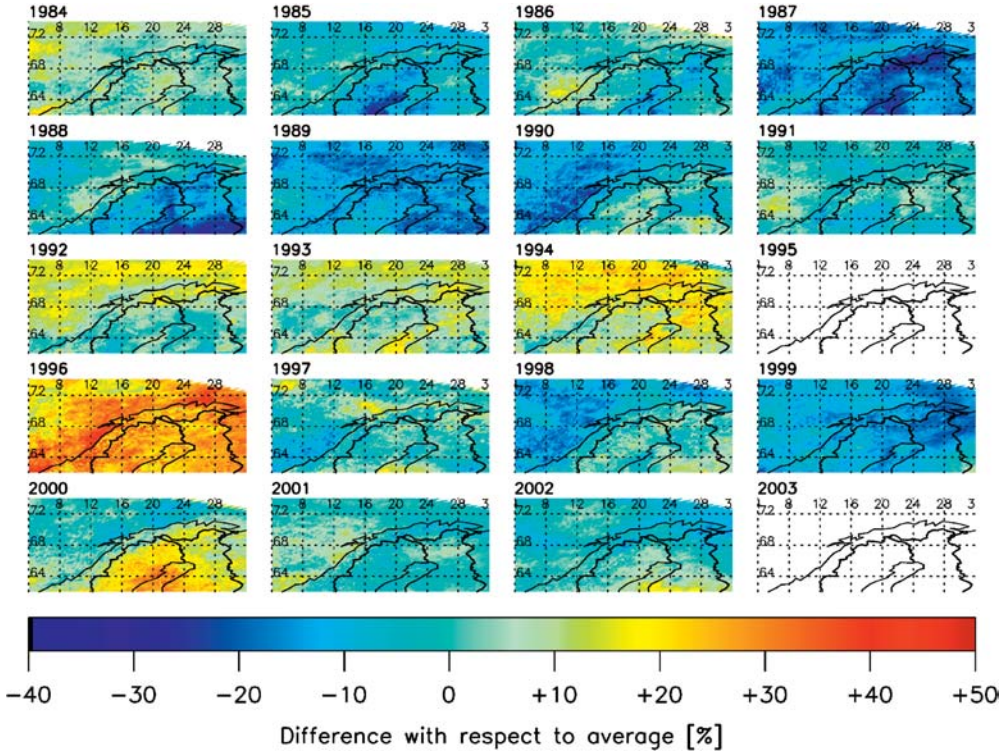

FIGURE 8. Sequence of maps showing the year-to-year variability of the monthly averaged daily erythemal dose in March over north Scandinavia/Finland (1995 is missing because of lacking ozone satellite data).

over the Nordic area in 1996 corresponds to very low ozone (~310 DU) with an about average cloudiness. Springtime is the period in the year that shows the largest year-to-year variability in surface UV radiation, due to the strongest variability in stratospheric ozone. This variability in ozone is also stronger at high latitudes. Deviations of up to ±30% are still found in summer, mostly due to the variability in cloudiness. The respective weight of ozone and cloudiness in the UV radiation variability is strongly dependent on the spectral range

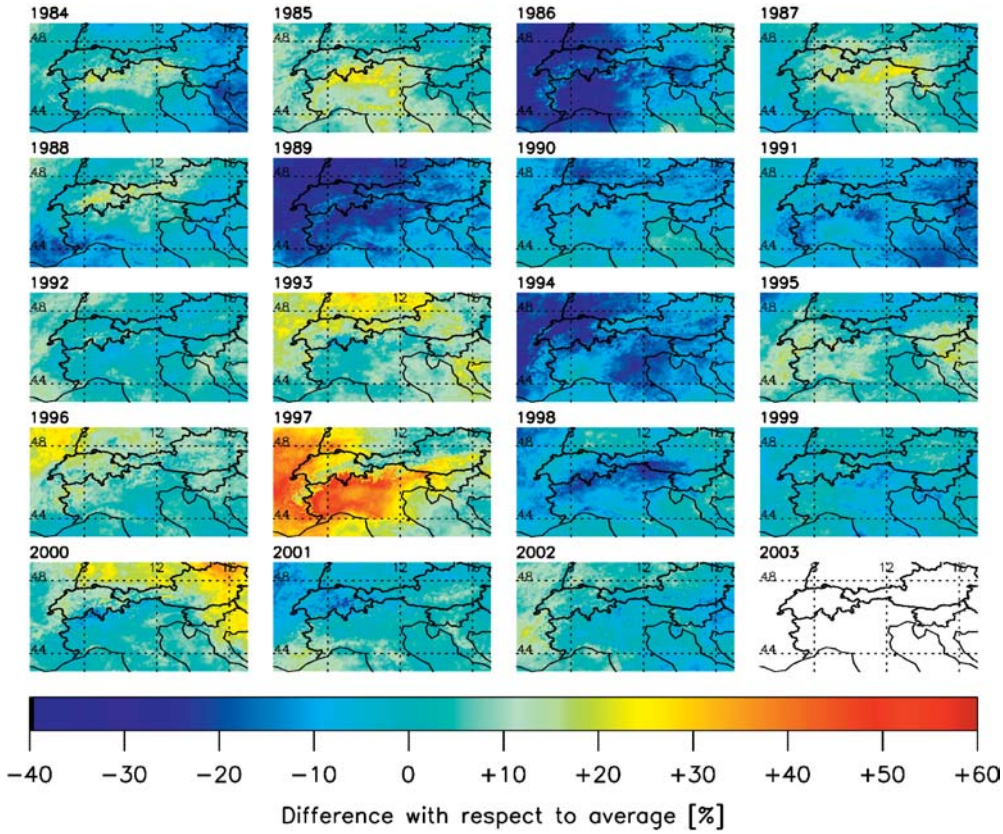

FIGURE 9. Sequence of maps showing the year-to-year variability of the monthly averaged daily erythemal dose in April over the alpine arc.

considered. UVA for instance is practically insensitive to ozone while, on the contrary, doses calculated with action spectra that put a heavy weight on the shorter wavelengths (such as the DNA damage action spectrum) are very sensitive to it. The erythemal dose is a medium case where ozone and cloudiness have roughly the same importance.

Conclusions

A satellite-derived climatology of the surface UV radiation over Europe is available for impact studies. It allows documentation of this environmental parameter where no measurements are or were available. It spans the period from 1984 to 2003 with daily maps and a spatial resolution of the order of 5 km. The quality of the satellite-derived estimates has been assessed at several sites in Europe. With a few exceptions, the bias of the satellite-derived erythemal daily doses with respect to the measurements is within the uncertainty of the absolute calibration of the ground instruments (±7%). The dispersion is large (~30% mean rms difference) but includes the intrinsic difference between a punctual measurement and the area average provided by the model. With its relatively high spatial resolution and time coverage, this climatological data set permits to document the spatial and temporal variability of the surface UV radiation with a level of details that enable impact studies. In particular, it reflects the effects of altitude, snow cover, and regional/local weather. The plans are to maintain, update, and upgrade this data set.

Acknowledgments

This work was supported under contracts No ENV4-CT97-0401 (MAUVE project) and No EVK3-CT-1999-00012 (UVAC project) of the RTD Programme of the European Commission. The author also wishes to thank EUMETSAT for providing the many METEOSAT images needed to perform this work and the MARS project of JRC for the gridded visibility data.

References Cited

Arola, A., Kalliskota, S., den Outer, P. N., Edvardsen, K., Hansen, G., Koskela, T., Martin, T. J., Matthijsen, J., Meerkötter, R., Peeters, P., Seckmeyer, G., Simon, P., Slaper, H., Taalas, P., and Verdebout, J., 2002: Four UV mapping procedures using satellite data and their validation against ground-based UV measurements. *Journal of Geophysical Research,* 107:ACL 11 1–11.

Bernhard, G. and Seckmeyer, G., 1999: Uncertainty of measurements of spectral UV irradiance. *Journal of Geophysical Research,* 104: 14321–14345.

Eck, T. F., Bhartia, P. K., and Kerr, J. B., 1995: Satellite estimation of spectral UVB irradiance using TOMS-derived ozone and reflectivity. *Geophysical Research Letters,* 22: 611.

Hansen, G., 2003: Final report of the project "The influence of UVR and climate conditions on fish stocks: a case study of the northeast arctic cod" (UVAC). Norwegian Institute for Air Research (NILU).

Krotkov, N. A., Bhartia, P. K., Herman, J. R., Fioletov, V., and Kerr, J., 1998: Satellite estimation of spectral surface UV irradiance in the presence of tropospheric aerosols–1. Cloud-free case. *Journal of Geophysical Research,* 103: 8779–8793.

Krotkov, N. A., Bhartia, P. K., Herman, J., Ahmad, Z., and Fioletov, V., 2001: Satellite estimation of spectral surface UV irradiance–2: Effect of horizontally homogeneous clouds and snow. *Journal of Geophysical Research,* 106: 11743–11759.

Lubin, D., Jensen, E. H., and Gies, H. P., 1998: Global surface ultraviolet radiation climatology from TOMS and ERBE data. *Journal of Geophysical Research,* 103: 26061–26091.

Mayer, B., Seckmeyer, G., and Kylling, A., 1997: Systematic long-term comparison of spectral UV measurements and UVSPEC modelling results, *Journal of Geophysical Research,* 102: 8755–8767.

McKenzie, R. L., Seckmeyer, G., Bais, A. F., Kerr, J. B., and Madronich, S., 2001: Satellite retrievals of erythemal UV dose compared with ground-based measurements at northern and southern midlatitudes. *Journal of Geophysical Research,* 106: 24051–24062.

Meerkötter, R., Wissinger, B., and Seckmeyer, G., 1997: Surface UV from ERS-2/GOME and NOAA/AVHRR data: A case study. *Geophysical Research Letters,* 24: 1939–1942.

Meerkötter, R., Verdebout, J., Bugliaro, L., Edvardsen, K., and Hansen, G., 2003: An evaluation of cloud affected UV radiation from polar orbiting and geostationary satellites at high latitudes. *Geophysical Research Letters,* 30: ASC 8-1–8-4.

Peeters, P., Müller, J.-F., Simon, P. C., Celarier, E., and Herman, J., 1998: Estimation of UV flux at the Earth's surface using GOME data. *ESA EOQ,* 58: 39–40.

Slaper, H., Velders, G. J. M., and Mattijsen, J., 1998: Ozone depletion and skin cancer incidence: a source risk approach. *Journal of Hazardous Materials,* 61: 77–84.

Verdebout, J., 2000: A method to generate surface UV radiation maps over Europe using GOME, Meteosat, and ancillary geophysical data. *Journal of Geophysical Research,* 105: 5049–5058.

Verdebout, J. and Vogt, P., 2001: Satellite derived UV maps over Europe: Method and application. *Proceedings of SPIE, 4428, Ultraviolet Ground and Space-based Measurements, Models and Effects*, 30 July–1 August, San Diego, USA, 240–248.

Ziemke, J., Chandra, S., and Herman, J., 2000: Erythemally weighted UV trends over northern latitudes derived from Nimbus 7 TOMS measurements. *Journal of Geophysical Research,* 105: 7373–7382.

Ms submitted February 2004